

“©2020 IEEE. Personal use of this material is permitted. Permission from IEEE must be obtained for all other uses, in any current or future media, including reprinting/republishing this material for advertising or promotional purposes, creating new collective works, for resale or redistribution to servers or lists, or reuse of any copyrighted component of this work in other works.”

# Robust Power Sharing between Dual Active Bridges to Improve a DC Microgrid's Stability

Dhiman Das  
Department of Electrical  
Engineering,  
IIT Delhi  
New Delhi, India  
dhiman.iitd@gmail.com

M. J. Hossain  
School of Electrical and Data  
Engineering  
University of Technology Sydney  
Sydney, Australia  
jahangir.hossain@uts.edu.au

Sukumar Mishra  
Department of Electrical  
Engineering,  
IIT Delhi  
New Delhi, India  
sukumariitdelhi@gmail.com

Bhim Singh, *Fellow, IEEE*  
Department of Electrical  
Engineering,  
IIT Delhi  
New Delhi, India  
bhimsinghiitd63@gmail.com

**Abstract**— The dual active bridge (DAB) is one of the key elements in different DC microgrid clusters. DAB also has isolation features and bi-directional power transfer capabilities between two power buses of similar or different levels, i.e. low voltage and high voltage buses. Due to the galvanic isolation and modularity nature of DAB, the output can be easily interconnected for efficient and reliable power sharing. In this paper, this advantage of modularity is applied in microgrid applications. A robust bi-directional power sharing control strategy is developed between DABs from different high voltage buses to low voltage buses in order to improve the voltage stability of the microgrid. The designed controller considering the non-linearity and uncertainty ensures stable DC bus voltage and reliable power sharing among DABs under different operating conditions.

**Keywords**— Dual Active Bridge, Microgrid, Power Sharing.

## I. INTRODUCTION

DC microgrids are getting popular as a cheaper and efficient alternative due to renewable sources, for example, photovoltaic (PV) units and wind turbines, integrations in low-voltage household networks. Moreover, most of the electric vehicles are to be charged overnight at the home, which have the vehicle to grid (V2G) and the grid to vehicle (G2V) capabilities. Many small size renewable generators produce low voltage DC power. It avoids the requirement of power conversions from DC to AC and makes the plug and play control viable. To connect EVs or DC type renewable sources, DABs can be used due to its bidirectional power transfer capabilities and isolation properties. However, accurate models and robust control algorithms are essential to achieve optimum performance from the DABs based DC microgrids.

As in the case of DC microgrid, the voltage on the line is related to power transfer to or from the network. So in order to balance this situation, ‘voltage balancing’ or ‘global voltage regulation’ is adopted by adjusting the power flow on

the network [1], [2]. A distributed control for average voltage regulation and current sharing based on the measurement of the generated current are proposed in [3] and verified with buck converter topology. A trust-based cooperative control is proposed in [4], where microgrid with a bus voltage of 48V is considered. It is shown that using information based on the local and neighbor node /converter, the false data injection attacks on the communication link can be mitigated. In [5], a distributed control technique of power sharing among different microgrid clusters, is proposed based on information gathered from the neighborhood cluster. Distributed control for voltage balancing with a non-isolated unidirectional DC-DC converter is proposed in [6]. A fully decentralized current control is proposed for a microgrid consisting of paralleled connected DC-DC converter in [7], where its dynamic model is developed, and the limitation of conventional droop control is addressed. The voltage control technique considering distributed energy sources with AC/DC interface is implemented in [8], and the linearized coupling model between DC voltage and AC frequency is addressed on the basis of virtual inertia. The DAB has enormous potential for several applications in DC microgrids; however, so far, its feasibility and control strategies are not investigated in detail.

This paper investigates the existing available models for multiple DAB-based DC microgrids and control strategies for their power sharing. A system is considered as shown in Fig. 1 where two DABs are interconnected at low voltage (LV) side and powered from different high voltage (HV) buses. These two DABs can be able to exchange bi-directional power from HV bus 1 to LV bus as well as HV bus 2 to LV bus. A robust power sharing algorithm is developed in order to maintain voltage stability of the buses and support power from both ends of DAB. This scheme of power sharing can help in the stability improvement of interconnected DC microgrid. As the power can be wheeled from one bus to

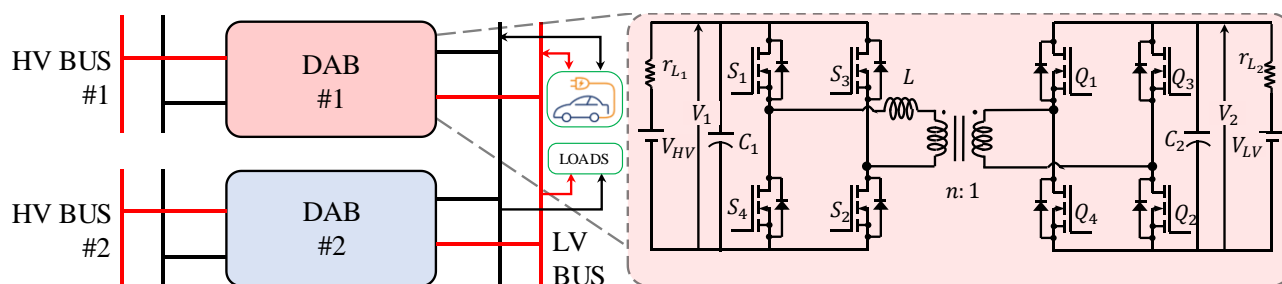


Fig. 1. Microgrid system with DAB converter.

another, so the stress on the main power grid also reduces in case of a vehicle to vehicle (V2V) power sharing.

## II. SYSTEM MODELLING

This section develops the nonlinear model of DABs, which is used to design the controller. Fig. 2(a) shows the different modes of operation DAB at steady state over a complete cycle. The power transfer of DAB is governed by [9],

$$P = \frac{V_{HV}V_{LV}}{2nf_sL}d(1-d) \quad (1)$$

where,  $d = \frac{\phi}{\pi}$  = phase shift ratio;  $V_{HV}, V_{LV}$  = voltages at high voltage side bridge and low voltage side bridge, respectively;  $f_s$  = switching frequency of the bridge;  $L$  = interfacing inductor between HV side bridge and transformer; and  $n$  = turns ratio of the transformer between two bridges.

Fig. 2(a) shows the switching sequence and different modes of operation for the DAB converter to flow power its HV side to LV side and describes the corresponding switching waveform. During mode 1,  $S_1$  &  $S_2$  (Fig.1) are turn on from HV side and  $Q_3$  &  $Q_4$  turn on at LV side. Because of the transformer action,  $n.V_{LV}$  voltage appears at the HV winding with reverse polarity, so there is an instantaneous voltage difference across the inductor  $L$  resulting in ramping up of the inductor current  $I_L$  as shown in Fig. 2. After a certain time, when the inductor current has reached desired peak value,  $Q_3$  &  $Q_4$  are turned off and  $Q_1$  &  $Q_2$  turn on as depicted in mode 2. The resultant time lag is converted to phase shift angle  $\phi$  with respect to the total time period  $T_s$ . As the voltage across the inductor is in the same phase,  $I_L$  ramps down slowly. If  $V_{HV}$  and  $V_{LV}$  are perfectly matched with the turns ratio ( $n:1$ ) i.e.  $V_{HV} = n.V_{LV}$ , then  $I_L$  is constant value i.e. parallel to the time axis. In mode 3, HV side bridge changes the voltage polarity of the inductor by turning off  $S_1$  &  $S_2$  and turning on  $S_3$  &  $S_4$  resulting in ramping down of  $I_L$ . As both the bridges are operated at 50% duty cycle,  $I_L$  ramps down to negative value up to angle  $\phi$ . During mode 4, LV side bridge changes its polarity and voltage across  $L$  appears at same phase resulting in  $I_L$  to ramp up. Thus, the principle of volt-second balance is maintained and power flows from HV side to LV side. In order to reverse power flow i.e. from the LV

side to HV side, the direction of  $\phi$  should be reversed with respect to HV side bridge voltage.

The amount of power transfer depends on the voltage magnitude between two buses and the angle difference between two bridges while other parameters remain fixed. Furthermore, the direction of the power transfer is also determined by the leading bridge to lagging bridge. So, the major factor of bidirectional power flow depends on the magnitude and direction of the phase difference between two bridges. Fig. 2(b) depicts the principle of DAB, experimentally verified at 60 kHz with a power level of 1 kW. The experimental parameters are given in Table I.

TABLE I. EXPERIMENTAL PARAMETRES

Sl. No.	Parameter		
	Description	Value	
1.	Series Inductor	Inductance	72.2 $\mu H$
		DCR	61m $\Omega$
2.	Transformer	Turns Ratio	5: 1
		Leakage inductance	49 $\mu H$
3.	Capacitor	HV Side	2 $\times$ 220 $\mu F$
		LV Side	8 $\times$ 470 $\mu F$
4.	Voltage	HV Side	250 V
		LV Side	48 V

The average small signal model of a single DAB converter, considering the line resistance ( $r_{L1}, r_{L2}$ ) as shown in Fig. 1 at the HV bus and LV bus and neglecting high frequency dynamics of inductor current can be given as [10],

$$\begin{bmatrix} \frac{d\langle v_1 \rangle}{dt} \\ \frac{d\langle v_{LV} \rangle}{dt} \end{bmatrix} = \begin{bmatrix} -\frac{1}{r_L C_1} & \frac{(D^2 - D)}{2Lf_s C_1} \\ -D^2 + D & -\frac{1}{RC_2} \end{bmatrix} \begin{bmatrix} \langle v_1 \rangle \\ \langle v_{LV} \rangle \end{bmatrix} + \begin{bmatrix} -\frac{1}{r_L C_1} & \frac{2D - 1}{2Lf C_1} \langle v_{LV} \rangle \\ 0 & -\frac{2D - 1}{2Lf C_2} \langle v_1 \rangle \end{bmatrix} \begin{bmatrix} \langle v_{HV} \rangle \\ \langle \Delta d \rangle \end{bmatrix} \quad (2)$$

Using the given model in (2), a model for two parallel DAB systems is developed with the system parameters, and finally,

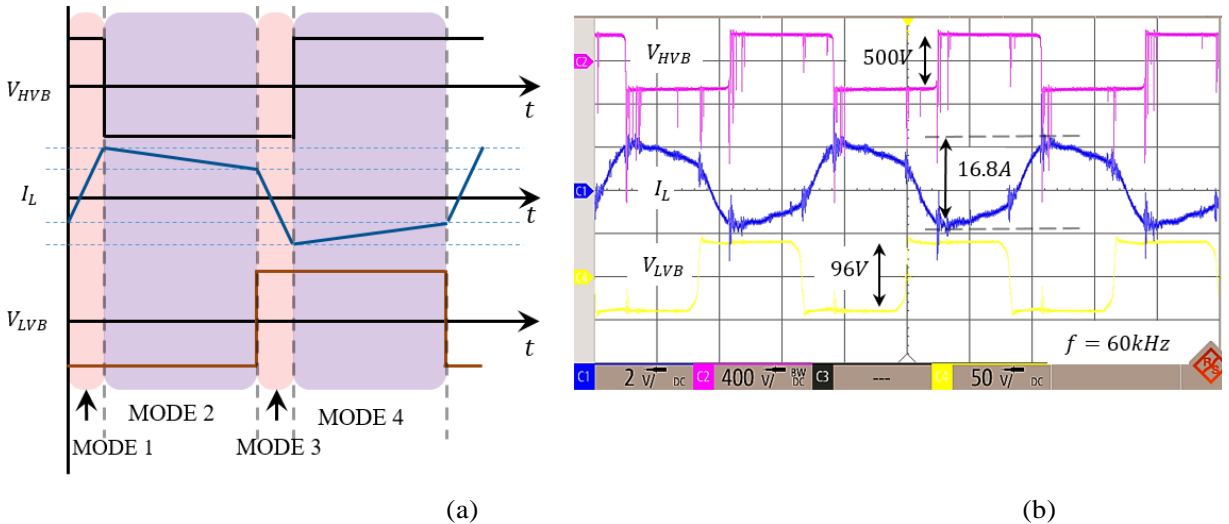


Fig. 2. Waveform of DAB converter (a) Theoretical, (b) Experimental for 1kW power transfer at 60 kHz from HV to LV.

the state space model is determined as per the parameter is given in Table I, as,

$$G(s) = \frac{\Delta V}{\Delta d} = \frac{156.508(s^2 + 500s + 2.67 \times 10^{10})}{(s + 45.48)(s^2 + 500s + 8.884 \times 10^9)} \quad (3)$$

### III. CONTROLLER DESIGN

For the design of the controller, the system needs to be linearized around the equilibrium point. In this paper, an improved linearized method is used, which represents the higher order terms of Tylor series as an uncertain terms and included in the controller design process. In order to design and to stabilize the controller for large disturbances around the equilibrium point, the right hand terms of the system differential equations (2) are expanded using Cauchy remainder formula for the Taylor series. The Cauchy remainder is considered as an uncertain parameter. The deviations of the operating point from the equilibrium point can be quantified by the uncertain parameter.

Fig. 3 depicts the control scheme of the system shown in Fig. 1. Measured variables such as voltage on both high side buses  $V_{HV1}, V_{HV2}$ , low voltage side bus  $V_{LV}$  and power on both the buses  $P_1, P_2$  are fed to the controller. In practical sense, the bus voltage of any microgrid is not stiff and has finite Thevenin's equivalent resistance, so by change in current at the buses results as the voltage fluctuations on the bus voltages. Moreover, bus voltage fluctuation is caused due to mismatch in the source power and load power requirement. Based upon the reference set for all the buses such as  $V_{HVref1}, V_{HVref2}, V_{LVref}$  the control action is taken and

amount of power is fed to the bus to maintain voltage stability. In this way, powers can be wheeled from HV bus 1 to HV bus 2 and it maintain the voltage stability of the all the buses of the microgrid.

Let  $(x_0, u_0)$  be any point of the system dynamics equation, using mean value theorem, the system equation can be rewritten as

$$\dot{x} = f(x_0, y_0) + L(x - x_0) + M(u - u_0) \quad (4)$$

where  $L = \left[ \frac{\partial f_1}{\partial x} \Big|_{x=x^*1, u=u^*1}, \dots, \frac{\partial f_4}{\partial x} \Big|_{x=x^*5, u=u^*5} \right]^T$ , and

$$M = \left[ \frac{\partial f_1}{\partial u} \Big|_{x=x^*1, u=u^*1}, \dots, \frac{\partial f_4}{\partial u} \Big|_{x=x^*5, u=u^*5} \right]^T.$$

Around  $(x_0, u_0)$ , providing disturbances, (4) can be written as follows

$$\Delta \dot{x} = \dot{x} - \dot{x}_0 = A\Delta x + (L - A)\Delta x + B_1\Delta u \quad (5)$$

Where,  $A = \frac{\partial f}{\partial x} \Big|_{x=x_0, u=u_0}$ ,  $B_1 = \frac{\partial f}{\partial u} \Big|_{x=x_0, u=u_0}$  and

$$\Delta x = [\Delta V_{HV1}, \Delta V_{HV2}, \Delta V_{LV}, \Delta P_1, \Delta P_2]^T$$

The value of  $(L - A)$  is difficult to obtain exactly, but possible to obtain a bound on  $\|(L - A)\|$ . The control scheme is shown in Fig. 3 and the system parameters are given in Table I. The value of  $(L - A)$  is computed based upon 10% change uncertainty and LQG controller is designed and bi-directional power flow can be controlled. The detail of control design process can be found in [5].

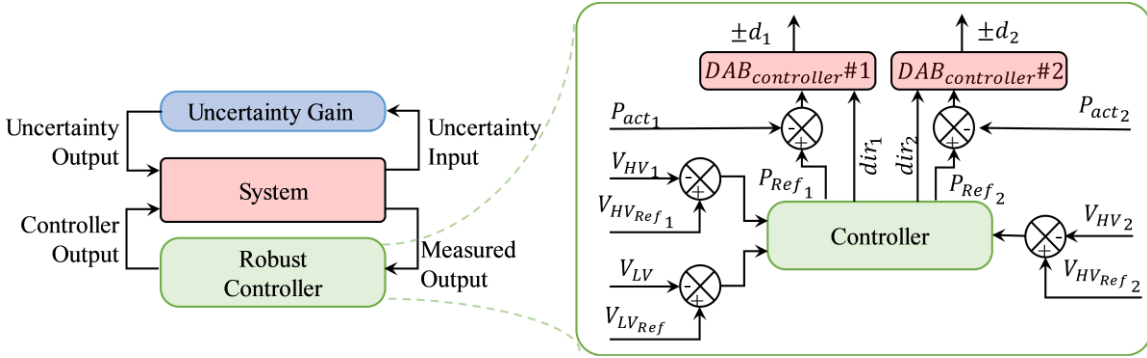


Fig. 3. Control architecture.

produces the required amount of power command for DABs. Now due to the bidirectional feature of DAB, power reference command can be bipolar in nature. If any bus voltage dips from the reference value then, the power has to supply to the bus and if the voltage rises at the bus the power has to extract from that bus. The amount of active power flow through the DAB depends upon the amount of phase shift as shown in Fig. 2(b). The direction of power flow is determined by leading or lagging bridge. The DAB controller produce the control output i.e phase shift ratio  $\pm d_1$  for DAB 1 and  $\pm d_2$  for DAB 2 based on the power reference with the direction. The

### IV. CONTROLLER VALIDATION

The controller design and different case studies are carried out using MATLAB. A simulation model is built based on the system of two parallel DAB as shown in Fig. 1 with the hardware parameters given in Table I. The simulation is carried out considering various possible conditions, and based on that controller performance is verified. Reference voltages  $(V_{LVref}, V_{HVref1}, V_{HVref2})$  as shown in Fig. 3, are set through the supervisory controller for the regulation of bus voltage. The current flowing out of the

bus is considered as +Ve value and the current entering the bus is considered as -Ve value.

#### A. Case 1. Failure of DAB Module

In case of failure of any DAB module, another DAB module participates in power flow to maintain the continuous flow of the power at the LV side bus. This scenario is depicted in Fig. 4, where power is flowing from LV bus to HV bus, and DAB-1 is considered as the failure. DAB-2 is turned on by the controller to maintain the uninterrupted power flow at the LV side. In Fig. 4, the voltage at the LV side is shown, which deviates due to the failure of DAB-1 and again restores due to turning on of DAB-2. This situation may also arise when source connected to the DAB-1 is interrupted. Due to modularity features and the proper control actions, the voltage of the bus is regulated to the desired value.

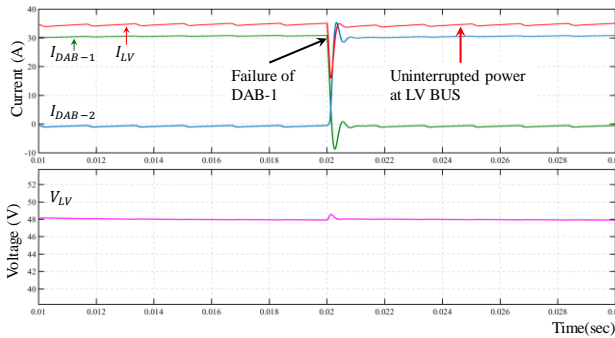


Fig. 4. Power flow of DAB at LV side in case of failure of DAB-1, DAB-2 participate in power sharing and uninterrupted flow of power is maintained at LV side.

#### B. Case 2. Both DAB Sharing The Power from the Same BUS:

In case of excessive power demand for a short duration of time, both DABs has to be turned on at the same time in order to avoid the voltage collapsing at the bus. In order to maintain the power demand and charge the bus voltage quickly the current is supplied into the bus at the same time through another DAB. This scenario is depicted in Fig. 5, where power flows from the LV side to both HV sides. DAB-2 is turned on while DAB-1 is already transferring power from the LV side to the HV side. So, the current at the LV bus is raised. DAB-2 is turned on to maintain the HV side 2 voltage and allows it to reduce the voltage up to 10% tolerance level. Fig. 5 shows the voltage level of different buses where LV side voltage is reduced to support the voltage level of the HV side 2 bus.

#### C. Case 3. Both DAB Sharing Power While Maintaining Bus Voltages at All Side:

In this scenario, both the DABs are sharing the power as well as regulating all the bus voltages to its set values. In this situation, two DAB may or may not share an equal amount of power but maintaining the voltage regulation is the primary objective of the controller. The amount of power sharing is set based upon the priority of availability of the sources. Fig. 6 depicts the control action taken by the controller under this situation. In Fig. 6, initially, the power flows from the LV bus to HV bus-1. DAB-2 is turned on to share the contribution of DAB-1, the current flowing through DAB-1 and DAB-2 at LV sides are shown. While DAB-2 is turned on, LV side current at DAB-2 is increased, to maintain the voltage at LV side, the phase shift ratio for DAB-1 is reduced; hence, the current at LV side of DAB-1 is also reduced. The voltages at

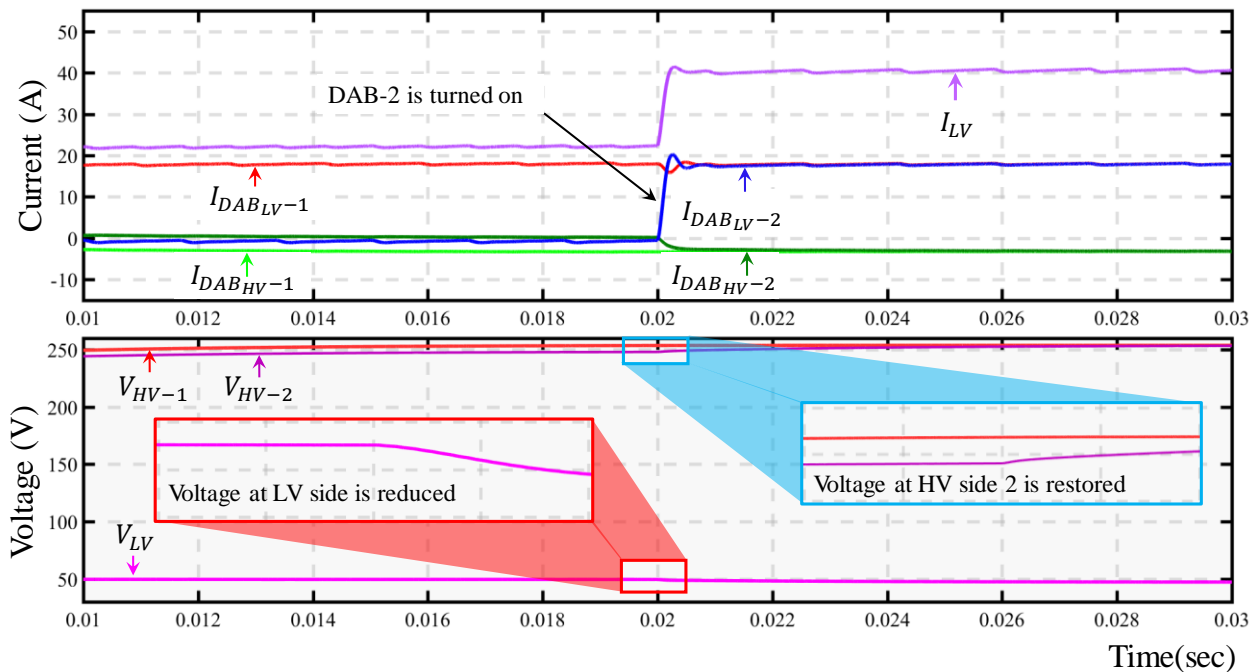


Fig. 5. Power sharing from the same bus with two DABs at the same time results voltage dip at the bus.



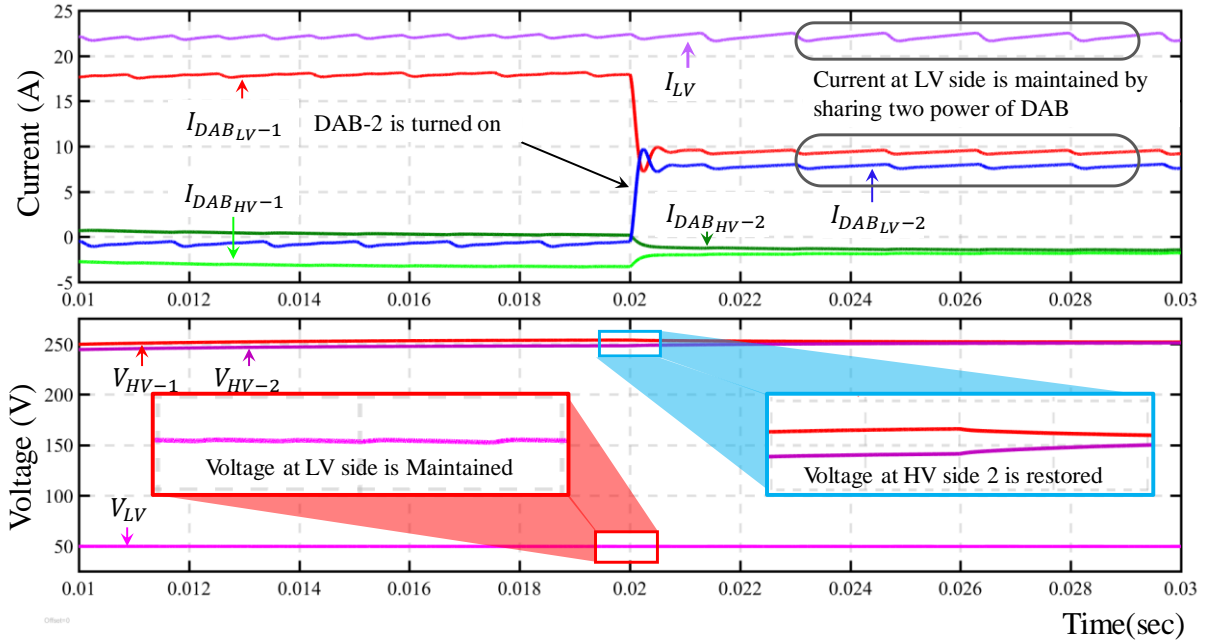


Fig. 6. Power sharing from the same bus with two DABs at the same time and maintained the bus voltage.

each bus are shown, where the LV side voltage is maintained as well as both the HV side bus voltages are restored to set its value. The power sharing is not equal here due to non-identical dynamics and uncertainty involved in both the HV buses. The controller is tuned such that, irrespective of external uncertainties, the bus voltage is regulated.

#### D. Case 4. Power Wheeling Between Two Different Buses:

In this scenario, the power can be wheeled for one bus to another bus by changing the direction of power flow. In this case, between HV side buses, without loading the LV side bus and the voltages at all the buses are also regulated. Fig. 7 depicts this situation; initially, power is flowing from HV side-1 to LV bus. LV side bus is supplied power to its load as well as takes power from DAB-1. The injected current is higher than the outgoing current to the load, so the current direction is -Ve in polarity. The voltage at the HV side-2 is below the reference voltage. The DAB-2 is turned on with the opposite direction, i.e. the direction of power flow from the LV side to HV side. With the contribution of DAB-2, the

power is transferred from the LV side to HV side-2. In Fig. 7, while DAB -2 is turned on, due to the power transfer from LV side to HV side-2, the current in the LV side bus changes its polarity to positive direction implies that this bus supplies the power to its connected local load. In order to maintain the bus voltages, the controller set the power command to the DAB-2 such that equal power can be drawn from HV side-1 and supplied to HV side-2. So, the direction of the current at the HV side-1 and HV side-2 is opposite but same in magnitude, as shown in Fig. 7. It reduces the loading of the LV bus. Due to the control action, the voltage of all buses is regulated as well as shown in Fig.7. Thus, the power is wheeled from HV bus-1 to HV bus-2 without a load LV bus. This strategy of power transfer can be applied to the vehicle to vehicle (V2V) application where two vehicles can exchange power in between them without loading the source or grid.

## V. CONCLUSIONS

A robust secondary voltage controller for a DC microgrid is designed and its performance is evaluated under different operating conditions. An improved linearized approach is used to linearize the system that retains the nonlinearity as an uncertainty. The inclusion of uncertainty improves the robustness of the closed loop system. The power sharing between DABs is conducted based on the priority of the available sources and loading conditions. The system's nonlinearities are considered in developing a robust control algorithm. The strategy assists the DABs to effectively control the DC bus voltage and share power among them depending on the loading conditions.

## REFERENCES

- [1] M. Tucci, L. Meng, J. M. Guerrero, and G. Ferrari-Trecate, "Stable current sharing and voltage balancing in DC microgrids: A consensus-based secondary control layer," *Automatica*, vol. 95, pp. 1–13, Sep. 2018.

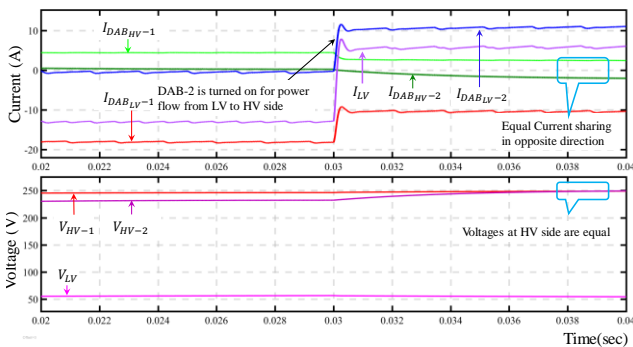


Fig. 7. Power wheeling from HV bus-1 to HV bus-2 without loading the LV side bus and maintaining voltages at every buses.

- [2] V. Nasirian, S. Moayedi, A. Davoudi, and F. L. Lewis, "Distributed cooperative control of DC microgrids," *IEEE Transaction on Power Electronics*, vol. 30, no. 4, pp. 2288–2303, Apr. 2015.
- [3] S. Trip, M. Cucuzzella, X. Cheng and J. Scherpen, "Distributed Averaging Control for Voltage Regulation and Current Sharing in DC Microgrids," *IEEE Control Systems Letters*, vol. 3, no. 1, pp. 174-179, Jan. 2019.
- [4] S. Abhinav, H. Modares, F. L. Lewis and A. Davoudi, "Resilient Cooperative Control of DC Microgrids," *IEEE Transactions on Smart Grid*, vol. 10, no. 1, pp. 1083-1085, Jan. 2019.
- [5] M. J. Hossain, M. A. Mahmud, F. Milano, S. Bacha and A. Hably, "Design of Robust Distributed Control for Interconnected Microgrids," *IEEE Transactions on Smart Grid*, vol. 7, no. 6, pp. 2724-2735, Nov. 2016.
- [6] M. Baranwal, A. Askarian, S. Salapaka and M. Salapaka, "A Distributed Architecture for Robust and Optimal Control of DC Microgrids," *IEEE Transactions on Industrial Electronics*, vol. 66, no. 4, pp. 3082-3092, April 2019.
- [7] E. Mojica-Nava, J. M. Rey, J. Torres-Martinez and M. Castilla, "Decentralized Switched Current Control for DC Microgrids," *IEEE Transactions on Industrial Electronics*, vol. 66, no. 2, pp. 1182-1191, Feb. 2019.
- [8] Y. Li, L. He, F. Liu, C. Li, Y. Cao and M. Shahidehpour, "Flexible Voltage Control Strategy Considering Distributed Energy Storages for DC Distribution Network," *IEEE Transactions on Smart Grid*, vol. 10, no. 1, pp. 163-172, Jan. 2019.
- [9] C. Mi, H. Bai, C. Wang, and S. Gargies, "The operation, design, and control of dual h-bridge based isolated bidirectional DC-DC converter," *IET Power Electron.*, vol. 1, no. 3, pp. 176–187, 2008.
- [10] H. Bai, C. Mi, C. Wang, and S. Gargies, "The dynamic model and hybrid phase-shift control of a dual-active-bridge converter," in *Proc. IECON 2008*, pp. 2840–2845.